Insight into tip vortex cavitation using velocity field measurements

Kyle M. Sinding, David R. Hanson, Michael H. Krane, and Jeremy Koncoski

Applied Research Laboratory, Penn State University, State College, PA, USA

Abstract

Statistics of tip vortex core pressure are estimated from instantaneous Stereo PIV measurements of the velocity field. The tip vortex was generated by a rectangular planform (aspect ratio 2), elliptically-loaded fin with a NACA66 foil shape. A set of 500 velocity field realizations were acquired at each of three angles of attack. Estimates of pressure for each measured velocity field were computed using a finite-element scheme that minimized error propagation from the measured velocity field. Histograms of core pressure show that the mean core pressure followed expected scaling with vortex strength, and that the width of the distribution is inversely proportional to vortex strength.

Keywords: tip vortex, cavitation, pressure estimation

Introduction

This paper presents estimates of tip vortex core pressure from instantaneous velocity fields measured in a plane intersecting a tip vortex (TV) flow over a rectangular planform. It has been proposed [1] that TV pressure coefficient fluctuations, relative to the mean, affect the mean incipient cavitation number. By non-intrusively acquiring a large number of velocity fields, and by estimating the pressure field associated with each [2], statistics of the TV pressure coefficient are derived.

Many studies have reported non-intrusive velocity measurements of a tip vortex flow over a stationary lifting surface [3-14,] but only a few include simultaneous velocity and load cell measurements [10-14]. Each study characterized vortex strength using velocity field measures, *e.g*., circulation, core radius, or core velocity profile shape. Of these, only Stinebring, *et al*., [9] estimated the vortex core pressure field using their velocity measurements. However, because the velocity field was measured point-by-point using Laser velocimetry, the pressure filed could only be estimated in an ensemble-averaged sense, and could only estimate an average departure from the mean using turbulent kinetic energy.

Here, a combination of load measurements and Stereo PIV measurements of velocity on a plane intersecting the TV are presented [14]. Using a finite element estimation technique [2], an instantaneous pressure coefficient, $C_{p,min}$, denoting pressure drop across the vortex core for each snapshot of the flow, was computed. From this ensemble of pressure coefficients, the probability density function and its first two moments (mean and standard deviation) are computed.

Methods

Flow measurements were conducted in the round test section of the 12inch water tunnel, located in Penn State Applied Research Laboratory's Garfield Thomas Water Tunnel facility [14, 15]. The tunnel test section flow speed ranges 0-80ft/s, and the independently controlled operating pressure ranges from 3-35psi, with free stream turbulence intensity to less than 0.5%. The tunnel test section is 18 inches long. The test section is optically accessible on three sides through flat, transparent acrylic windows. The fourth side is composed of a base plate on which the fin is mounted. A rectangular planform (aspect ratio 2) fin generated the tip vortex. The fin had a NACA 66(mod) profile and a spanwise twist distribution giving elliptical loading profile, and a rounded tip. The quarter chord was centered on the fin base/load cell axis of rotation.

Twenty-four pressure taps are located along the test section, between each window/baseplate, at 6 axial locations. A Kiel probe, located in the plenum, was used to measure total pressure. All pressures were measured using Heise DXD series, 100 PSIA digital pressure transducers. Tunnel speed was estimated using the total pressure, test section entrance pressure, and the cross section areas of the tunnel at the pressure probe locations. An AMTI Model MC1-6-250-5763

*Corresponding Author, Michael Krane: mhk5@arl.psu.edu

six-axis load cell measured the forces and moments applied to the fin during the experiment. Load cell strain gage voltages, all tunnel pressures, and water temperature data were all recorded digitally with a National Instruments DAQ system.

As illustrated in Figure 1, Stereo Particle Image Velocimetry (SPIV) measurements were performed on a plane oriented at a right angle to the tunnel axis, roughly centered on the location of the tip vortex, approximately 0.50 chord lengths downstream of the trailing edge. The plane was illuminated with a dual head Nd:YAG Solo PIV laser, operated in double pulse mode, at a frequency of 15Hz. Images were captured with two Sensicam cameras operating in doubleshutter mode. A combination of LaVision Scheimpflug lens mounts and acrylic prisms pressed onto the window exterior minimized optical distortion. The spatial calibration was performed using a 200mm^2 dual-plane, dual-side calibration target (TSI, Inc.) with markers spaced vertically and horizontally 10mm apart, and a 1mm displacement between planes. Image pairs were acquired using INSIGHT 3G software (TSI, Inc.) and processed using standard, multipass stereo-cross-correlation software (DAVIS 8.0.5, LaVision). In the final pass, a 32x32 pixel correlation window, with 50% overlap, was used, resulting in a 19x33 point vector field (627 total vectors) over the field of view.

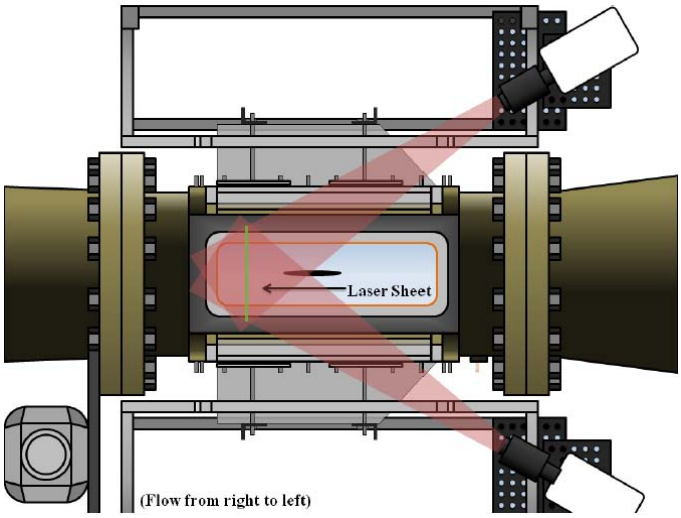

Figure 1. Schematic of SPIV setup, showing cameras, optical path (pink), prisms (gray) imaging laser sheet (green), and fin [14]. Flow is from right to left.

An instantaneous pressure field was estimated from each velocity field acquired, using a finite element formulation [2]. This method reduces the error propagation from the measured velocity into the estimated pressure field, and allows for more flexibility in applying pressure boundary conditions on the region containing the measured velocity field. The pressure and pressure gradient on the border of the measurement region was estimated using the velocity field. Finite-differencing of the velocity field was used to estimate the normal pressure gradient, at all but one point on the boundary, where the pressure was estimated using the total pressure measured in the plenum, and the measured local velocity vector, and the Bernoulli equation. This point was chosen such that it was the least likely to be located on a streamline that had passed through an upstream region containing vorticity. For each vector field, a pressure coefficient is defined in terms of the difference between minimum core pressure and ambient pressure:

$$C_{p,min} = \frac{p_{min} - p_\infty}{\frac{1}{2}\rho {U_\infty}^2}$$

Results

Velocity was measured in a plane located one half chord downstream of the trailing edge, nominally centered on the tip/trailing edge corner location, at U_∞ = 30 ft/s, for three angles of attack ($\alpha = 0^o$, $\alpha = 2.5^o$, and $\alpha = 5^o$). At each angle of attack, 500 image pairs were acquired. For each resulting velocity field snapshot a corresponding pressure field was computed as described above. A typical result is shown in Figure 2. The minimum pressure coefficient $C_{p,min}$ was then computed from each field.

Figure 3 shows tip vortex pressure difference statistics as a function of tip vortex strength. Figure 3a shows probability density functions of $-C_{p,min}$ for each of the three angle of attack conditions tested. Figure 3b shows variations of the mean and standard deviations of $-C_{p,min}$as a function of tip vortex strength $C_L^2 Re^{0.4}$ [see, *e.g.*, 16]. These results show that mean vortex core pressure coefficient increases, while variations about that mean decrease, with angle of attack (vortex strength). These results indicate that the minimum core pressure variation can be higher than 10% of the mean.

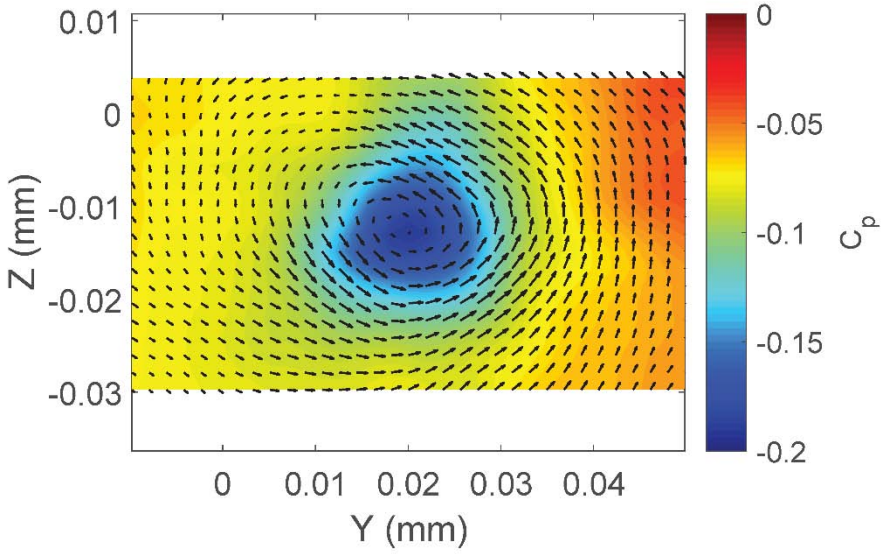

Figure 2. Instantaneous snapshot of velocity and pressure fields of tip vortex, measured one-half chord length downstream of fin trailing edge. $\alpha = 0^o$, $U_\infty = 9.2$m/s. Vectors show velocity projected onto measurement plane, colormap shows pressure coefficient.

Summary

This paper presents statistics of tip vortex core pressure, estimated from instantaneous velocity measurements in a plane intersecting the vortex core. The vortex was generated using an elliptically-loaded fin. Pressure estimation was performed using a finite element scheme that minimizes propagation of velocity error into the pressure estimation. For the three fin angles of attack studied, pressure statistics were presented. These show that the mean core pressure coefficient follows the expected trend with vortex strength, and that the variations of core pressure relative to the mean have an inverse proportionality with vortex strength.

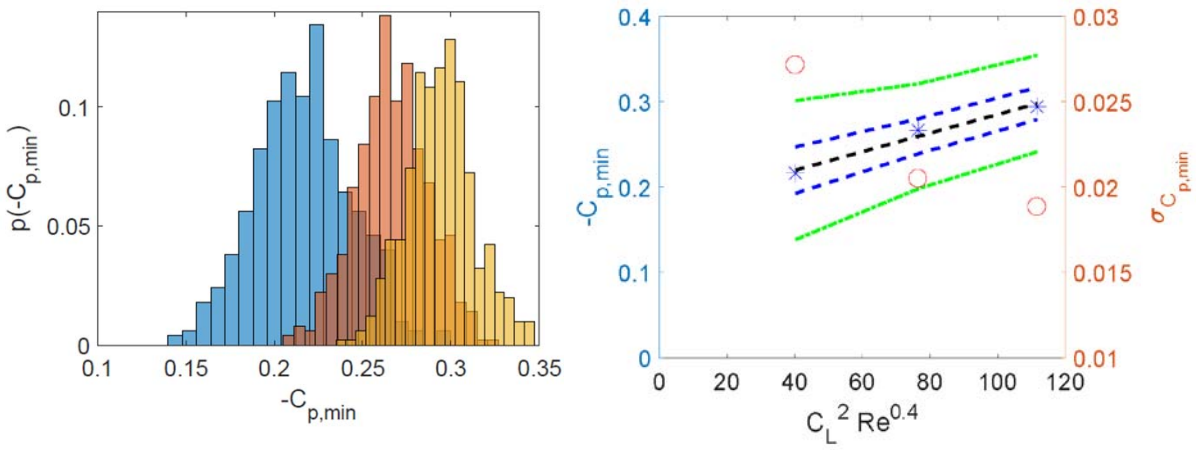

(a) *(b)*

Figure 3. Tip vortex core pressure statistics as a function of tip vortex strength. *(a)* Probability density functions of $-C_{p,min}$ for the three test conditions: *blue*: $\alpha = 0^o$, *pink*: $\alpha = 2.5^o$, *yellow*: $\alpha = 5^o$. *(b)* variation with tip vortex strength ~ $C_L^2 Re^{0.4}$: *: mean $-C_{p,min}$, o: standard deviation of $-C_{p,min}$. Blue and green lines indicate one and two standard deviations from the mean, respectively. Note that as vortex strength increases, the mean core pressure difference increases, and the variation of core pressure difference decreases.

References

[1] R.E. Arndt, A.P. Keller (1992) *Water quality effects on cavitation inception in a trailing vortex*, Journal of Fluids Engineering, Transactions of the ASME 114(3), 430.
[2] Krittian, S., Lamata, P., Michler, C., Nordsletten, D., Bock, J., Bradley, C., Smith, N. (2012). *A finite-element approach to the direct computation of relative cardiovascular pressure from time-resolved MR velocity data*, Medical Image Analysis, 16, 1028.
[3] A. Shekarriz, J. Katz, H. Liu, T. Huang, T. Fu (1992) *Study of Junction and Tip Vortices Using Particle Displacement Velocimetry,* AIAA Journal 30(1), 145.
[4] A. Shekarriz, T. Fu, J. Katz, T. Huang (1993) *Near-field behavior of a tip vortex,* AIAA Journal 31(1), 112.
[5] A. Vogt, P. Baumann, J. Kompenhans, M. Gharib (1996) *Investigations of a wing tip vortex in air by means of DPIV,* in Advanced Measurement and Ground Testing Conference, p. 2254.
[6] B.S. Thurow, T. Fahringer, K. Johnson, S. Hellman (2014) *Comparison of plenoptic PIV and stereo PIV measurements in a wing tip vortex,* in The International Symposia on Applications of Laser Techniques to Fluid Mechanics, Lisbon, Portugal.
[7] Birch, D., Lee, T., Mokhtarian, F., Kafyeke, F. (2003) *Rollup and near-field behavior of a tip vortex*, Journal of Aircraft 40(3), 603.
[8] Zhang, H., Zhou, Y., Whitelaw, J. (2006) *Near-field wing-tip vortices and exponential vortex solution*, Journal of Aircraft 43(2), 445.
[9] Stinebring, D., Farrell, K., Billet, M. (1991) *The structure of a three-dimensional tip vortex at high Reynolds numbers*, Journal of Fluids Engineering 113, 496.
[10] Beresh, S., Hening, J., Spillers, R. (2009) *Planar velocimetry of a fin trailing vortex in subsonic compressible flow*, AIAA Journal 47(7), 1730.
[11] Beresh, S., Smith, J., Hening, J., Grasser, T., Spillers, R. (2009) *Interaction of a fin trailing vortex with a downstream control surface*, Journal of Spacecraft and Rockets 46(2), 318.
[12] Elsayed, O. Asrar, W., Omar, A., Kwon, K. (2011) *Evolution of NACA23012 wake vortices structure using PIV*, Journal of Aerospace Engineering 25(1), 10.
[13] Krane, M., Meyer, R., Weldon, M., Elbing, B., DeVilbiss, D. (2015) *Measurements of loading and tip vortex due to high-Reynolds number flow over a rigid lifting surface*, Journal of Fluids Engineering 137(7), 071301.
[14] Hanson, D. (2012) *Cavitation inception for non-elliptically loaded fins*. M.S. thesis, The Pennsylvania State University.
[15] Lauchle, G. Billet, M., Deutsch, S. *High-Reynolds number liquid flow measurements,* in Frontiers in Experimental Fluid Mechanics, vol. 46, ed. by M. Gad-el Hak (Springer).
[16] Arndt, R. (2002) *Cavitation in vortical flows*, Annual Review of Fluid Mechanics, 34, 143.